

# A numerical model of the $M_2$ tide in the Gulf of St. Lawrence

Gulf of St. Lawrence  
Numerical Model  
Mixing  
Tidal Fronts

Golfe du Saint-Laurent  
Modèle numérique  
Mélange  
Fronts de marée

R. D. Pingree<sup>a</sup>, D. K. Griffiths<sup>b</sup>

<sup>a</sup> Institute of Oceanographic Sciences, Wormley, Surrey, U.K.

<sup>b</sup> The Laboratory, Marine Biological Association, Citadel Hill, Plymouth, U.K.

Received 28/6/79, in revised form 11/10/79, accepted 11/12/79.

## ABSTRACT

A two-dimensional numerical model of the  $M_2$  tide in the Gulf of St. Lawrence and the St. Lawrence Estuary is developed in spherical polar coordinates. The model is used to predict frontal regions separating areas of tidally mixed waters from areas showing pronounced summer stratification. Marked increases in biological productivity may be associated with upwelling and mixing in these regions.

*Oceanol. Acta*, 1980, 3, 2, 221-225

## RÉSUMÉ

Un modèle numérique de la marée  $M_2$  dans le golfe du Saint-Laurent.

Un modèle numérique bidimensionnel de la marée  $M_2$  dans le golfe du Saint-Laurent et dans l'estuaire du Saint-Laurent est développé en coordonnées polaires sphériques. Le modèle est utilisé pour prédire l'emplacement des zones frontales qui séparent les régions verticalement homogènes, des régions où existe une stratification estivale. Une augmentation notable de la productivité biologique peut être associée à la remontée, et au mélange des eaux, dans ces régions.

*Oceanol. Acta*, 1980, 3, 2, 221-225.

## INTRODUCTION

A numerical model of the  $M_2$  tide in the Gulf of St. Lawrence is developed and described in order to determine the effects of tidal mixing on the vertical structure of the water column. The Gulf of St. Lawrence was chosen to represent a region of generally low tidal mixing. A further model has been derived for the Ungava Bay, Hudson Strait and Foxe basin system as representative of a strong tidal environment (Griffiths *et al.*, 1981). Interdisciplinary studies have shown that tidal mixing can have a marked effect on temperature structure and hence phytoplankton distributions (Pingree, 1978 *a*). These models together with a model of the North West European Shelf (Pingree, Griffiths, 1978) are intended to form the basis for making comparative studies of phytoplankton in widely differing geographical regions. Additional effects due to wind driven currents will be considered in a further paper.

## THE EQUATIONS OF MOTION

A two-dimensional model of the Gulf of St. Lawrence and the St. Lawrence Estuary was developed, using the fully non-linear form of the hydrodynamic equations. The depth-averaged equations of continuity and momentum may be written in spherical polar coordinates as follows:

(a) Continuity

$$\frac{\partial E}{\partial t} + \frac{1}{R \cos \varphi} \times \left[ \frac{\partial}{\partial \lambda} (h+E)u + \frac{\partial}{\partial \varphi} (h+E)v \cos \varphi \right] = 0; \quad (1)$$

(b) Momentum:

(i) in the east direction

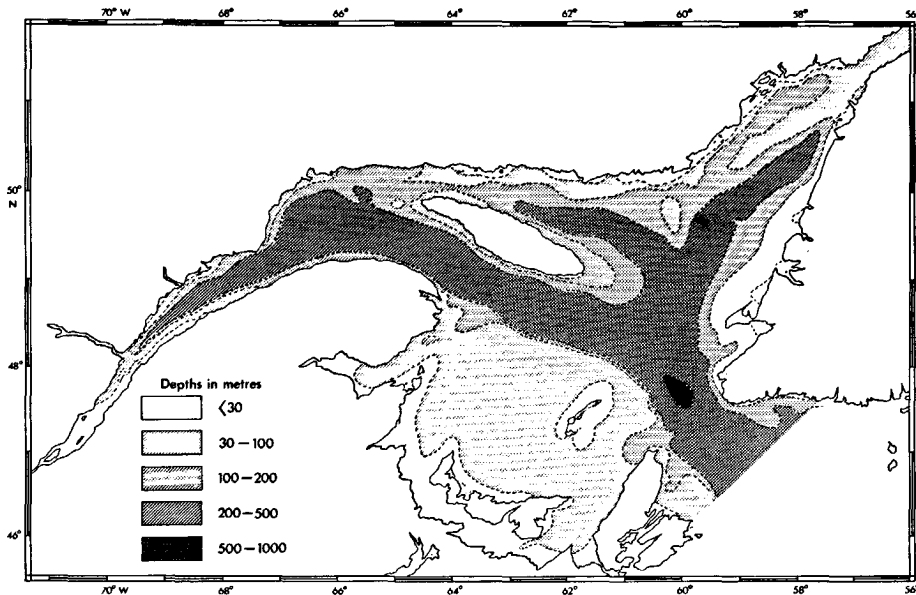


Figure 1  
The Gulf of St. Lawrence and St. Lawrence Estuary showing water depth contours in metres.

$$\begin{aligned} \frac{\partial u}{\partial t} + \frac{u}{R \cos \varphi} \frac{\partial u}{\partial \lambda} \\ + \frac{v}{R} \frac{\partial u}{\partial \varphi} - \frac{uv}{R} \tan \varphi - 2 \Omega \sin \varphi v \\ = \frac{-g}{R \cos \varphi} \frac{\partial E}{\partial \lambda} - \frac{\tau_\lambda}{\rho(h+E)} + \text{TGF east}; \end{aligned} \quad (2)$$

(ii) in the north direction

$$\begin{aligned} \frac{\partial v}{\partial t} + \frac{u}{R \cos \varphi} \frac{\partial v}{\partial \lambda} \\ + \frac{v}{R} \frac{\partial v}{\partial \varphi} + \frac{u^2 \tan \varphi}{R} + 2 \Omega \sin \varphi u \\ = \frac{-g}{R} \frac{\partial E}{\partial \varphi} - \frac{\tau_\varphi}{\rho(h+E)} + \text{TGF north}. \end{aligned} \quad (3)$$

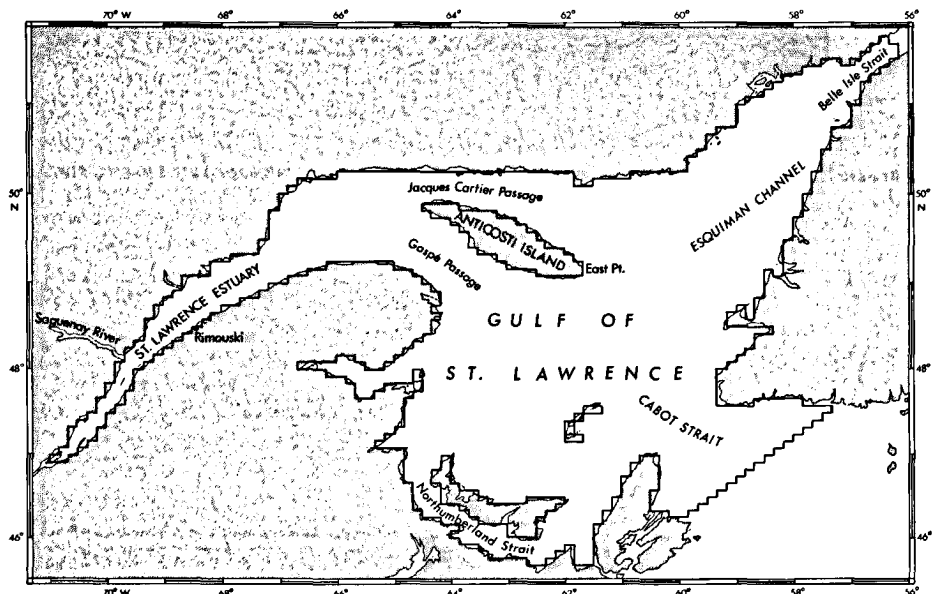
The symbols are defined in the Table.

The bottom stress  $\tau_B$  is defined in terms of its components in the east direction,  $\tau_\lambda$ , and north direction,  $\tau_\varphi$ .

Thus

$$\tau_B = \tau_\lambda \mathbf{i} + \tau_\varphi \mathbf{j}. \quad (4)$$

Figure 2  
The grid for the numerical model and place names mentioned in the text.



TGF denotes the tide generating force and the direct tide generating forces were applied over the modelled region according to the formulae

$$\begin{aligned} \text{TGF east} \\ = \frac{-Ag}{R} \cos \varphi \sin(\sigma t + 2\lambda), \end{aligned} \quad (5)$$

TGF north

$$= \frac{-Ag}{R} \cos \varphi \sin \varphi \cos(\sigma t + 2\lambda), \quad (6)$$

with  $A=48.8$  cm (see Hendershott, Munk, 1970; Hamblin, 1976).

### THE NUMERICAL MODEL

The modelled region (Fig. 1) was divided by a grid lattice of 5' in latitude (5 nautical miles) and 10' in longitude giving  $\sim 3 \times 10^3$  sea grid points where both tidal elevations and tidal currents could be determined (Fig. 2). The numerical scheme uses the staggered mesh and leap-frog method with linear numerical analogues centred in space and time (Pingree, Griffiths, 1978, 1979).

The M<sub>2</sub> tidal forcing of the model is provided by two sources, externally by boundary values and directly by the tide generating force. The open sea boundary elevations at the entrance to Cabot Strait and the Strait of Belle Isle were specified in the form

$$E(t) = H \cos(\sigma t - g_E),$$

where  $t$  is the time after the passage of the moon over the Greenwich meridian and  $H$  and  $g_E$  are tidal constants for the M<sub>2</sub> tidal elevation  $E(t)$  with frequency,  $\sigma$ , obtained from published data (Farquharson, 1962; Dohler, 1966).

In partially enclosed shelf seas the tide generating force is usually sufficiently small that it can be neglected in comparison to the tide driven externally at the open sea boundaries. However in the weak M<sub>2</sub> tidal environment of the Gulf of St. Lawrence (with tidal current amplitudes generally less than 20 cm.s<sup>-1</sup>) a 5° bias in M<sub>2</sub> phase was removed by including the tide generating force. The non-linear terms although small, were also retained so that tidal residuals and harmonics could subsequently be examined.

Bottom friction is generally expressed in the quadratic form:

weak M<sub>2</sub> currents. A related form for the bottom friction was also used

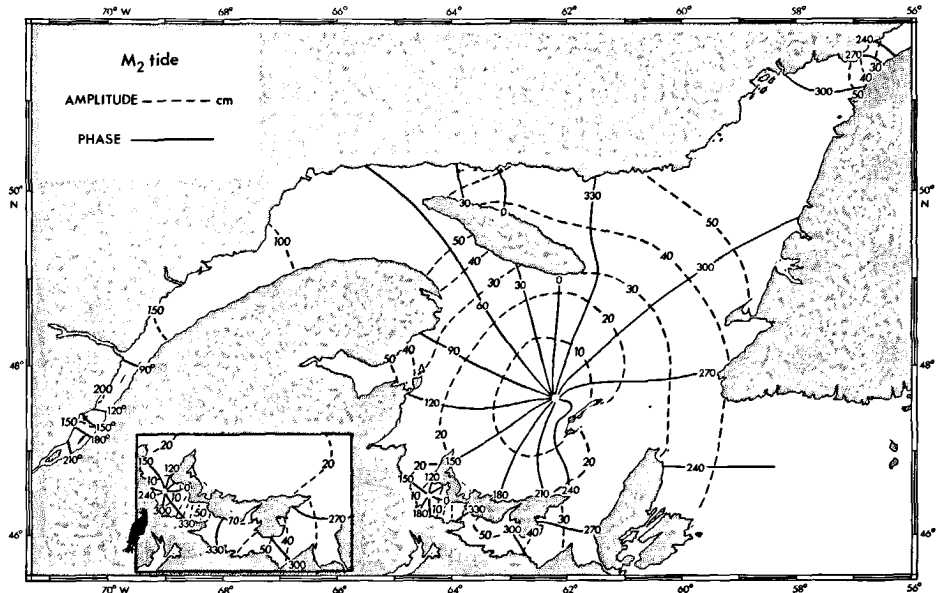
$$\tau_B = \varphi C_D (|\mathbf{u}| + s) \mathbf{u}. \quad (10)$$

The output from the numerical model was Fourier analysed to determine the M<sub>2</sub> tidal elevations and phases on each grid square. The co-phase lines are given for time zone (GMT + 4) hours following previous presentations for this region based on observational data (Farquharson, 1962; Dohler, 1966). The phase and amplitude values [shown in Figure 3 using (10) with  $s = 20 \text{ cm.s}^{-1}$ ] agree with published data for coastal stations with a standard deviation of 8 cm in amplitude and 10° in phase. Slightly improved amplitude values were obtained in the Northumberland Strait using (9) (see inset in Figure 3) but the overall standard deviations were not significantly improved.

The vector currents were also analysed to derive the tidal ellipse properties and these are available for comparisons with real data.

In one run of the model the effect of closing the Strait of Belle Isle with a land boundary was investigated.

Figure 3  
The M<sub>2</sub> cotidal chart derived from the numerical model. Phase values,  $g_E$ , are presented relative to time zone (GMT + 4) hours.



$$\tau_B = \rho C_D \mathbf{u} |\mathbf{u}|, \quad (8)$$

where  $C_D = 0.0025$  is the drag coefficient, and  $\mathbf{u}$  is the M<sub>2</sub> tidal current. Such a form for the bottom friction may be far from ideal if other components of the kinetic energy spectrum have comparable energy. For example, in regions of low M<sub>2</sub> tidal current, bottom friction based on (8) may be seriously underestimated. Ideally the model should include other important tidal constituents and perhaps wind stress so that these currents can contribute to the bottom friction. As a practical expedient the bottom stress was linearised for speeds less than  $s$  such that

$$\begin{aligned} \tau_B &= \rho C_D \mathbf{u} |\mathbf{u}| & \text{for } |\mathbf{u}| > s \\ \text{and} \\ \tau_B &= \rho C_D s \mathbf{u} & \text{for } |\mathbf{u}| < s. \end{aligned} \quad (9)$$

A "background" current speed,  $s \sim 20 \text{ cm.s}^{-1}$  was found to allow satisfactory dissipation in regions of

Near resonance conditions in the Esquiman Channel were obtained with the M<sub>2</sub> tidal amplitude increasing from  $\sim 25$  to 160 cm at the imposed barrier. The phase was retarded to 340°.

### TIDAL MIXING, FRONTS AND UPWELLING

The local mean dissipation of energy,  $e$ , per unit area in the numerical model due to work done against bottom friction is simply the scalar product of the bottom stress and the tidal velocity averaged over time

$$e = \overline{\tau_B \cdot \mathbf{u}}. \quad (11)$$

If this value is divided by the mass of the water column,  $\rho h$ , the tidal energy dissipation rate per unit mass,  $\epsilon$  ( $\text{cm}^2 \cdot \text{s}^{-3}$ ) is obtained. The reciprocal of this value in C.G.S. units expressed as a logarithm to base 10 is essentially the Simpson-Hunter (1974) stratification parameter,  $S$ , where

$$S = -\log_{10} \epsilon. \quad (12)$$

Contours of  $S$  evaluated from the  $M_2$  tidal model are illustrated in Figure 4. Studies in other areas dominated by the  $M_2$  tide (Pingree, Griffiths, 1978) have demonstrated that values of  $S$  in the neighbourhood of  $S \sim 1.5$  define transitional regions between waters that are well mixed,  $S < 1$ , and waters that are well stratified,  $S > 2$ , during the summer months. Contributions from other semidiurnal constituents ( $S_2, N_2$ ) are already implied in this choice of  $S$  and as a result of stored buoyancy minimal frontal movement is anticipated during the springs to neaps cycle of tidal mixing. It should be remembered that for a change of  $S$  from 1 to 2 an order of magnitude change in  $\epsilon$  occurs and so frontal prediction using (9) instead of (10) gives essentially similar results particularly where the gradients of  $S$  are well-defined. In some regions the diurnal currents can be important and ideally this constituent should have been included.

There are also important non-tidal currents in the Gulf of St. Lawrence that will affect the  $S$  values locally which are not covered in this particular analysis and such pronounced oceanographic features as the Gaspé current (El-Sabh, 1976) can on occasions be conspicuous in infrared imagery. Marked baroclinic instability in this region of the Gaspé Passage can be seen in the infrared image illustrated in Figure 5. Dramatic upwelling events are also sometimes evident along the northern Quebec coastline. However, a feature which is perhaps less conspicuous, but nevertheless relatively persistent, is the localised cooling in the Jacques Cartier Passage between Anticosti Island and the northern Quebec coastline (see Fig. 5). Reference to Figure 4 shows that this is clearly a frontal region due to tidal mixing. The numerical model also indicates that the cool feature stretching from the mouth of the Saguenay River towards I du Bic near Rimouski is also likely to be of tidal origin despite the expected additional surface buoyancy input due to fresh water run off which may partially suppress mixing in these estuarine conditions. Further significant numerical predictions for tidally mixed regions (where  $S < 1.5$ ) occur in the Strait of Belle Isle and the Northumberland Strait.

From dynamical considerations all promontories and narrows are likely to show locally increased tidal mixing. In very weak tidal environments complete tidal mixing may not occur. However the reduced stability associated with promontories may still favour these regions, in preference to adjacent very stable areas, as key upwelling sites, whether due to wind or tidal effects (Garrett, Loucks, 1976). Thus some features which appear of marginal significance based on the stratification criterion may still be quite important. Such an example may occur at East Point, Anticosti Island where the model (Fig. 4) indicates weaker stability but not necessarily well mixed conditions although cool water can clearly be observed (Fig. 5).

## DISCUSSION

Earlier tidal models of the St. Lawrence Estuary (see Levesque, 1977 for a bibliography) have been extended to cover the whole of the Gulf of St. Lawrence region. The numerical model is derived in spherical polar coordinates and includes the direct effect of the tide generating force.

The  $M_2$  tide in the Gulf of St. Lawrence is generally small with tidal amplitudes less than 50 cm and associated tidal currents less than  $20 \text{ cm.s}^{-1}$ . However, in narrow straits and off promontories tidal streaming may increase locally and predictions based on the stratification parameter indicate that well mixed conditions can occur in the summer months. Examples of such effects can be observed in the Jacques Cartier Passage, the Northumberland Strait and the Strait of Belle Isle.

In the St. Lawrence Estuary the tidal regime becomes marked with  $M_2$  tidal elevations reaching 2 m. As the tidal streams increase in amplitude toward the head of the estuary and the water depth becomes shallower a marked change from stratified to mixed conditions occurs in the neighbourhood of the Saguenay River.

Although many of these frontal regions may be too small to show the characteristic eddies that have occasionally been observed along the more extended frontal

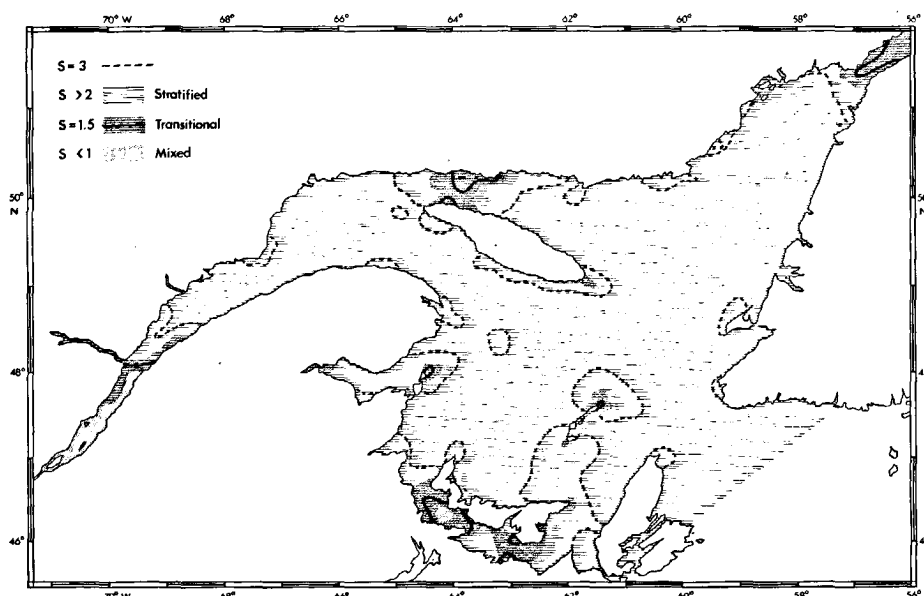


Figure 4  
Contours of the stratification parameter  $S$  with bold line ( $S = 1.5$ ) identifying frontal regions.



Figure 5  
NOAA 5 infrared image  
(5 August 1978) showing  
tidally mixed regions in  
the Jacques Cartier  
Passage.

boundaries around the North West European Shelf (Pingree, 1978) it seems likely that they will be important biologically in determining increased local mixing and sites for upwelling.

#### Acknowledgements

This work was done following a suggestion of Dr. M. Sinclair of the Bedford Institute of Oceanography, and we thank him for his help in setting up the numerical model. Dr. M. El Sabh of SOUQAR provided the hydrographic maps of the modelled region and Mr G. A. W. Battin kindly prepared the illustrations.

Table

Symbols used in the text

$t$	time coordinate
$E$	surface elevation
$h$	undisturbed water depth
$R$	radius of the Earth
$\lambda$	longitude-east
$\phi$	latitude
$E$	$M_2$ tidal elevation
$\mathbf{u}$	velocity with components $u, v$ in the east and north directions respectively
$C_D$	drag coefficient = 0.0025
$g$	acceleration due to gravity
$s$	speed
$S$	Stratification parameter
$e$	energy dissipation per unit area
$\epsilon$	energy dissipation per unit mass
$\Omega$	angular velocity of the Earth rotation
$\sigma$	$M_2$ angular frequency
$\tau_B$	bottom drag with components $\tau_x, \tau_y$
$\rho$	density of sea water
$\bar{\quad}$	overbar, denotes time average over one complete tidal cycle
$\mathbf{i}$	unit vector in the east direction
$\mathbf{j}$	unit vector in the north direction

#### REFERENCES

- Dohler G. C., 1966. Tides in Canadian Waters, Canadian Hydrographic Service, Marine Sciences Branch, Department of Energy, Mines and Resources, Ottawa, Cat. No. M54-966.
- El Sabh M. I., 1976. Surface Circulation Pattern in the Gulf of St. Lawrence, *J. Fish. Res. Board Can.*, **33**, 124-138.
- Farquharson W. I., 1962. Tides, Tidal streams and Currents in the Gulf of St. Lawrence, Marine Science Branch, Department of Mines and Technical surveys, Ottawa, 76 p.
- Garrett G. J. R., Loucks R. H., 1976. Upwelling along the Yarmouth shore of Nova Scotia, *J. Fish. Res. Board Can.*, **33**, 116-117.
- Griffiths D. K., Pingree R. D., Sinclair M., 1981. Summer Tidal Fronts in the near Arctic regions of Foxe Basin and Hudson Bay, *Prog. Oceanogr.* (in press).
- Hamblin P. F., 1976. A theory of short period tides in a rotating basin, *Philos. Trans. R. Soc., London, ser. A*, **281**, 97-111.
- Hendershott M., Munk W., 1970. Tides, *Ann. Rev. Fluid Mech.*, **2**, 205-244.
- Levesque L., 1977. Étude du modèle mathématique de la propagation des marées dans l'Estuaire du Saint-Laurent, Souqar. Université du Québec à Rimouski, 161 p.
- Pingree R. D., 1978 a. Mixing and stabilisation of phytoplankton distributions on the North West European Shelf, in: *Spatial Pattern in Plankton Communities*, edited by J. H. Steele, Plenum Press, 470 p.
- Pingree R. D., 1978 b. Cyclonic Eddies and cross frontal mixing, *J. Mar. Biol. Ass. U. K.*, **58**, 955-963.
- Pingree R. D., Griffiths D. K., 1978. Tidal fronts on the shelf seas around the British Isles, *J. Geophys. Res.* (Oceans and Atmospheres), Chapman Conference Special Issue, **83**, 4615-4622.
- Pingree R. D., Griffiths D. K., 1979. Sand Transport paths around the British Isles resulting from  $M_2$  and  $M_4$  tidal interactions, *J. Mar. Biol. Ass. U. K.*, **59**, 497-513.
- Simpson J. H., Hunter J. R., 1974. Fronts in the Irish Sea, *Nature*, London, **1250**, 404-406.

